Bull. Mater. Sci., Vol. 13, Nos 1 & 2, March 1990, pp. 121–133. © Printed in India.

High electron mobility transistors

S SUBRAMANIAN
Tata Institute of Fundamental Research, Bombay 400 005, India

Abstract. In this article, I briefly review the physics of the high electron mobility transistor (HEMT), the technological steps involved in the fabrication of the device, the current status, the remaining problems, and some areas of active research in which new developments might be expected in the future.

Keywords. High electron mobility transistors; *p*-modulation doping; inverted HEMT; double heterojunction HEMT; molecular beam epitaxy; velocity modulation transistor.

1. Introduction

The high electron mobility transistor (HEMT) is one of the fastest operating transistors on the scene today. Switching speeds (≈ 10 ps) with very low power dissipation (≈ 10 fJ) have been demonstrated using this device (Solomon and Morkoc 1984). The device operates on the principle that free carriers (electrons/holes) can move much faster in an undoped semiconductor than in a doped sample of the same material, since the scattering of the free carriers by the ionized impurities is much less in the former. However, in a bulk semiconductor, it is impossible to introduce free carriers without sharing the same volume with ionized impurities. The very clever idea that the physical separation of the free carriers from the parent donor/acceptor impurities might be possible using the built-in fields at the heterojunction interfaces was first realised by Esaki and Tsu (1969) in their pioneering work on superlattices. The actual effect, however, was first demonstrated by the Bell Laboratories group (Dingle *et al* 1978), using a GaAs/AlGaAs superlattice in which only the AlGaAs layers were selectively doped and the GaAs layers were undoped. This resulted in a transfer of electrons from the AlGaAs to GaAs, leaving behind the ionized donors in AlGaAs, the consequence of which was clearly seen in the dramatic increase in the measured electron mobility of this structure, as compared to the mobility in a bulk GaAs sample, especially at low temperatures ($T < 100$ K). Dingle *et al* (1978) named this technique "modulation doping", and it was soon realized that this effect can be utilized to make fast transistors, using a single modulation-doped heterojunction structure, rather than a modulation-doped superlattice. The realization of such a transistor was soon reported by several groups (Morkoc 1981; Judaprawira *et al* 1981; Mimura *et al* 1981; Linh *et al* 1982; Dilorenzo *et al* 1982; Lee *et al* 1983a) and the device was given different names, such as, modulation-doped field effect transistor (MODFET), transferred electron gas FET (TEGFET), selectively doped heterojunction transistor (SDHT) etc. Since then, this device has attracted the attention of a number of research groups around the world, and a large number of papers have been published during the last eight years, covering the various aspects of the device. It is impossible (neither is it my intention here) to cover all these developments in a brief review. On the other hand, I will try to present a comprehensive account of the basic physics and technology underlying the different aspects of the device to give a

flavour of the field. For a more exhaustive treatment of the subject, the reader is referred to the several excellent review articles already published (Solomon and Morkoc 1984; Morkoc 1985). The organization of the paper is as follows: Section 2 describes how the device is fabricated, § 3 deals with the important aspects of the device physics, and in §§ 4 and 5 the remaining problems, the new developments, the areas of active research, and the new proposed structures are briefly discussed.

2. Device fabrication

As mentioned in § 1, HEMT is fabricated from a single heterojunction structure of GaAlAs/GaAs in which only the AlGaAs layer is selectively doped. A typical cross-section of the device structure is shown in figure 1. It consists of an undoped GaAs buffer layer (≈ 1 μm), an undoped $Al_xGa_{1-x}As$ spacer layer (≈ 40–100 Å), a Si-doped $Al_xGa_{1-x}As$ layer (400–500 Å), and finally a GaAs cap layer (≈ 100 Å) also Si-doped, grown sequentially on a semi-insulating GaAs substrate, either by molecular beam epitaxy (MBE) or metal organic chemical vapour deposition (MOCVD). The AlAs mole fraction in the $Al_xGa_{1-x}As$ layers (x) is usually $\approx 0{\cdot}3$. This composition has been found to be the optimum from the following considerations. For smaller values of x the conduction band discontinuity at the heterojunction is smaller and hence the concentration of the electrons collected in the resulting potential well also decreases (discussed in more detail in § 3). For larger values of x the problems due to traps (the so-called DX centers) become more severe (discussed in § 4). The doping concentration in the Si-doped AlGaAs, as well as in the top GaAs cap layer is made as high as possible, and it is usually in the range of 1–2×10^{18} cm^{-3}. For this reason, Si is chosen as the dopant in preference to other donors like Sn, which have a tendency to segregate near the surface at high concentrations. The purpose of the GaAs cap layer is to protect the easily oxidizable surface of the AlGaAs layer until the device is ready for further processing. The undoped GaAs buffer layer is of either conductivity type n^- or p^-, with the unintentional doping concentration in the range of 10^{13}–10^{14} cm^{-3}. In the case of MBE growth, it is p^- (believed to be due to carbon), and it is n^- in the MOCVD grown structures. The growth temperature is usually in the range of 600–650°C in the case of MBE growth.

Once the device structure is grown, the transistor can be fabricated by a simple 3-step procedure using conventional photolithographic techniques. The first step is to

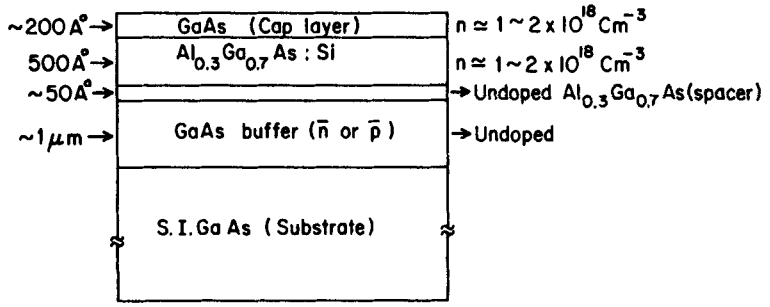

Figure 1. Schematic typical cross-section of an AlGaAs/GaAs HEMT structure.

define islands containing the individual devices and etch mesas (reaching down to semi-insulating substrate) in a cool $3H_2SO_4 : H_2O_2 : H_2O$ solution for about 30 s to achieve isolation between the devices. The second step is to print the source drain ohmic contact pattern, and transfer this pattern to evaporated Au-Ge Ni by the standard lift-off technique, and alloy the ohmic contact in an H_2 atmosphere for about 2 min at $\approx 480°C$. The last step is to print the gate pattern and transfer this pattern to the gate metal (usually Al or TiPdAu) again by the lift-off technique. A brief recess etching of the gate areas using $50H_2O : 3H_3PO_4 : 1H_2O_2$ is usually done just before the gate metal is evaporated. The duration of the recess etching is in the range of 30 to 90 s to control the threshold voltage of the device, and thus normally-on or normally-off transistors can be fabricated. A flow chart illustrating the fabrication procedure described above and a schematic of the cross-section of a finished device ready for testing are shown in figure 2. The mask-set used by us in the above fabrication procedure was designed to include the following test devices; two short length transistors (gate lengths of 2·5 and 5 μm), a fat transistor (gate length $\approx 75\,\mu$m), gated Van der Pauw geometry, a capacitor, and a transmission line geometry for contact resistance measurements. A photomicrograph of a finished test pattern fabricated on an HEMT structure is shown in figure 3. Typical drain characteristics (and the corresponding transfer characteristics) of a depletion mode HEMT (fat transistor) having a pinch off voltage $\approx -0{\cdot}35$ (fabricated by us) are shown in figure 4.

3. Device physics

3.1 *Formation of the 2-DEG channel*

The band diagram of the device structure shown in figure 2, in the growth direction z is shown in figure 5a. In order to understand why the bands bend in a complicated manner as shown in this figure, it is instructive to look at the band diagram (shown in figure 5b) of bulk AlGaAs and GaAs, in a hypothetical situation in which the two materials are isolated. If we let the two materials come in contact, and if we assume that the transition from AlGaAs to GaAs is abrupt (in the scale of atomic dimensions), then the sharp change in the band gap from AlGaAs to GaAs results in discontinuities in the conduction and the valence bands, as shown in figure 5a. Further, since the Fermi energies in the two materials are different, the electrons diffuse from AlGaAs to GaAs until the Fermi levels are lined up to restore equilibrium. This leaves behind the positively charged ionized donors in AlGaAs and the resulting strong electric field produces a severe band bending in GaAs, forming a narrow quasi-triangular potential well which confines the electrons to a very thin region (≈ 100 Å) inside GaAs close to the heterojunction interface. The spatial confinement of the electrons in the direction within a distance comparable to the de Broglie wavelength of the electron quantizes the electron motion in that direction, whereas in the layer plane, the electrons are described by the regular Bloch states in GaAs. The two-dimensional character of the electrons near the interface has been well-established by the Shubnikov de Haas oscillations (Stormer *et al* 1979), and hence the electron gas confined in the quasi-triangular potential well near the heterojunction interface is often referred to as the 2-dimensional electron gas (2DEG).

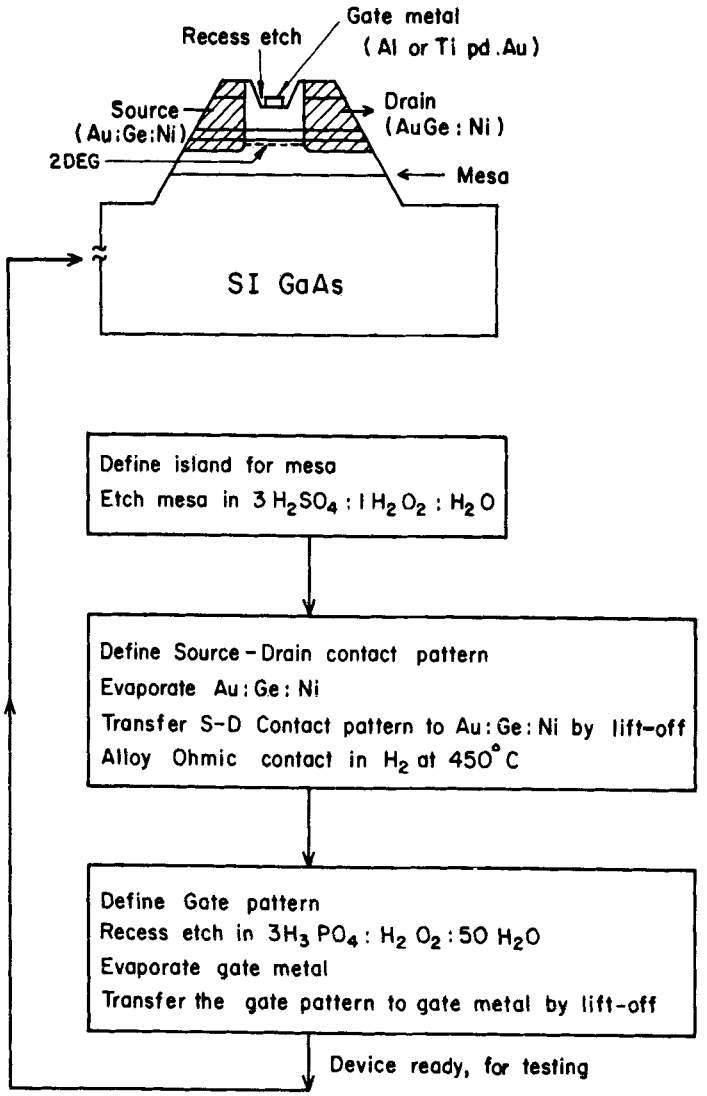

Figure 2. Flow chart showing the typical steps involved in the fabrication of HEMT using standard photolithography techniques and a schematic of the cross-section of a finished device ready for testing.

3.2 *Charge concentration of the 2-DEG*

The quasi-triangular potential well described above is a dynamic well in the sense that the potential profile of the well is determined by the charge concentration contained in it (through the Poisson equation), whereas the charge concentration itself is determined by the solution of the Schrodinger equation taking into account the potential profile of the well. Thus, the 2-DEG concentration has to be obtained by the self-consistent solution of the Poisson and Schrödinger equations (Vinter 1984). The problem is often simplified by making the triangular potential approximation for the well (for which the Schrödinger equation can be solved

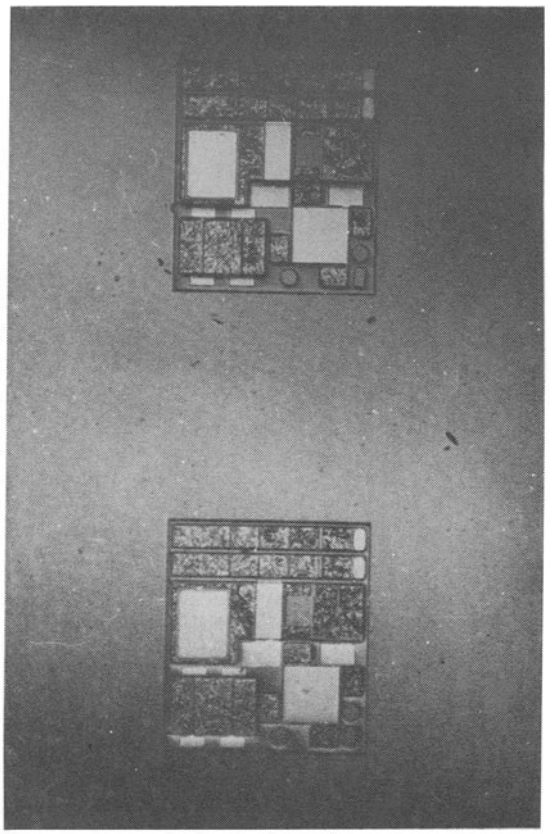

Figure 3. Photomicrograph of a typical test pattern fabricated in our laboratory on an HEMT structure.

analytically), and solving the Poisson equation analytically under the depletion approximation (Delagebeaudeuf and Linh 1982; Lee *et al* 1983b). However, the self consistency between the two solutions can be ensured only by a successive numerical iteration procedure. The experimental values of the charge concentration, however, seem to have a better fit with the calculations based on a fully consistent solution, taking into account both the shallow and deep donors in AlGaAs (Subramanian *et al* 1986). If the charge concentration is not too large, so that the electron occupation in all the higher sub-bands in the well except the first one may be neglected, the variational approach has also been found to be quite satisfactory (Hirakawa *et al* 1984).

3.3 *Charge control*

The charge concentration of the 2-DEG discussed in § 3·2 refers to the maximum charge the well can hold for the given device parameters. The charge control, for the operation of the device, is achieved by the application of a bias to the Schottky barrier gate placed on the Si-doped AlGaAs. It was mentioned in § 2 that the Si-

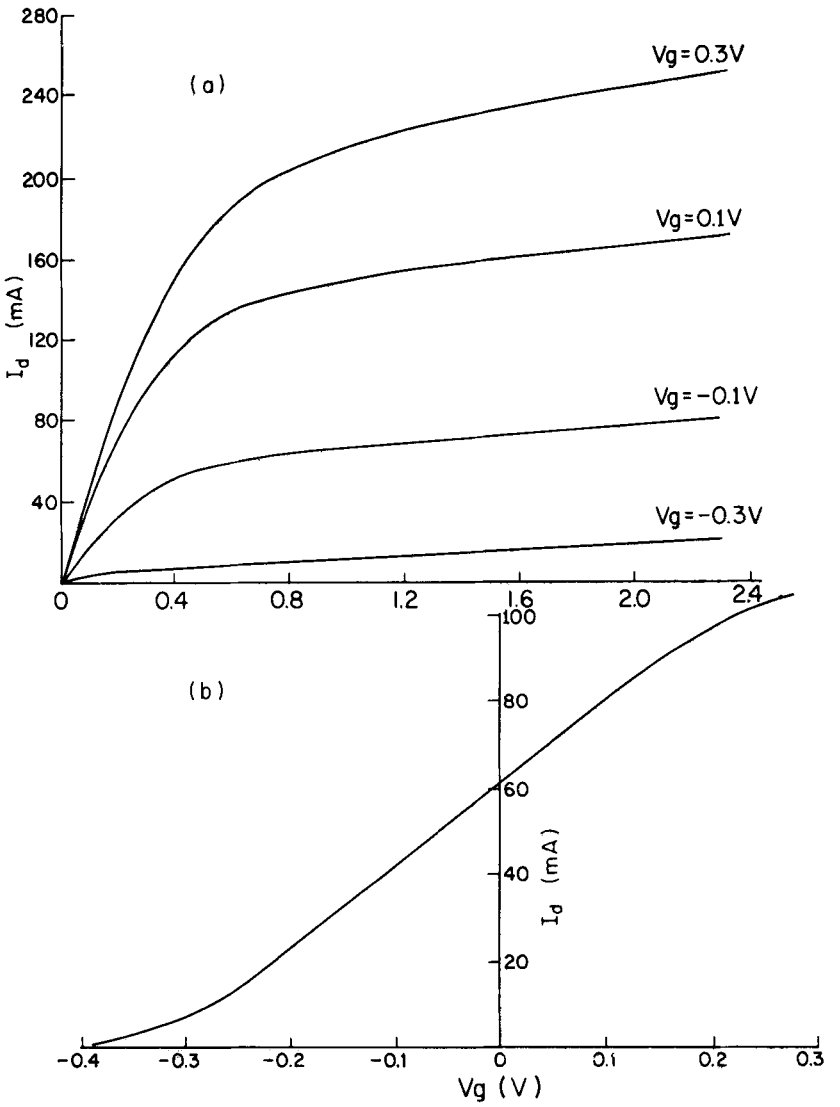

Figure 4. Drain (**a**) and transfer (**b**) characteristics of a typical normally-on HEMT fabricated in our laboratory. The ordinate for both (**a**) and (**b**) is the drain current (I_d). The abcissa for (**a**) is the source to drain voltage (V_d) and that for (**b**) is the source to gate voltage (V_g).

doped AlGaAs layer is recess-etched to a desired thickness before the evaporation of the Schottky gate metal. If the thickness of the AlGaAs region is sufficiently large such that there is no overlap of the depletion regions due to the Schottky junction and the heterojunction, at zero gate bias, a normally-on device is formed (figure 6a). In the normal operation of an HEMT, a device is never operated in the regime shown in figure 6a, as it contains a parallel conducting channel in the AlGaAs with a much poorer mobility (parasitic MESFET effect). When a negative gate bias is applied to this device, the Schottky junction depletion region starts overlapping

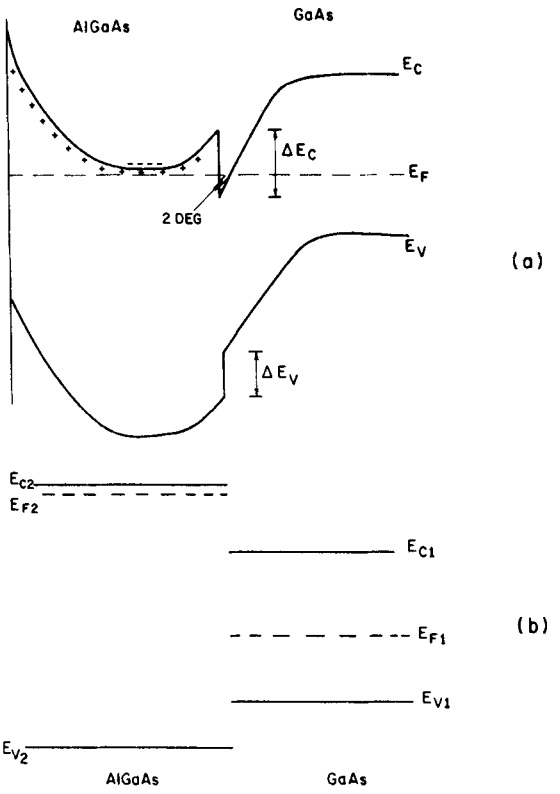

Figure 5. (**a**) Band diagram of an HEMT in the growth direction. (**b**) Band diagram near AlGaAs/GaAs junction when the two materials are not in actual contact.

with the heterojunction depletion region, and the charge control action starts (figure 6b). The charge concentration in the channel decreases as the gate voltage is made more negative, and the channel gets completely pinched-off for a sufficiently large negative bias (figure 6c). If, on the other hand, the thickness of the AlGaAs left after recess-etching is sufficiently small, then the channel may be pinched-off even at zero bias by the Schottky barrier potential itself. The charge can be added to the channel by the application of a positive bias to the gate. A device operating in this mode is called normally-off transistor (figures 6d and 6e). Detailed expressions for the charge control, drain I–V characteristics, the transconductance etc can be found in a number of papers in the literature (Delagebeaudeuf and Linh 1982; Drummond *et al* 1982; Lee *et al* 1983c, d). In both the normally-on and normally-off transistors, in the charge-control regime, the Si-doped AlGaAs is completely depleted and simply acts like an insulator. Thus, the device action in an HEMT is very much analogous to that of a Si-MOSFET, and this correspondence permits one to use directly the MOS formalism in modelling HEMT with appropriate change in notation (Pierret and Lundstrom 1984).

3.4 *Carrier mobility in the channel*

The mobility of the carriers in the channel is mainly determined by the polar optic

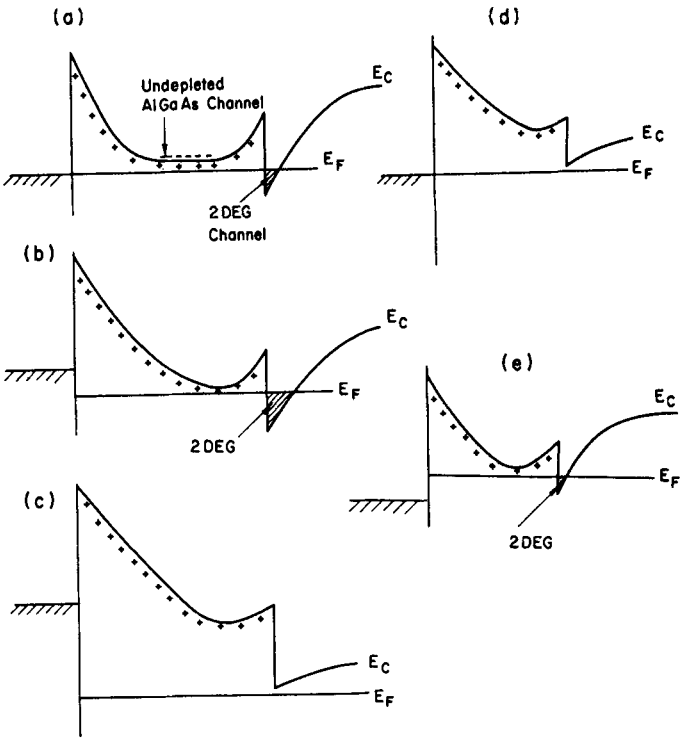

Figure 6. Different modes of operation of HEMT: Parasitic MESFET regime (**a**), charge-control regime (**b**) and pinch-off regime (**c**) for a normally-on device, and pinch-off regime (**d**) and charge-control regime (**e**) for a normally-off device.

scattering at higher temperatures ($T > 250$ K) and at higher fields, while at low temperatures the coulomb scattering of the (remote) impurities plays major role. The purpose of the undoped AlGaAs spacer layer is to keep the electrons in the channel farther from the impurities in the Si-doped AlGaAs. Thus the mobility can be increased by increasing the spacer layer thickness (Drummond *et al* 1981), but at the expense of decreasing the net electron concentration accumulated in the channel (Drummond *et al* 1983). The trade-off between the mobility and the charge concentration limits the spacer thickness to typically ≈ 50 Å for best results. The carriers are also subjected to a small amount of impurity scattering due to the background impurities in the channel and in the spacer regions. However, this impurity scattering is strongly screened by the large concentration of electrons in the channel. Thus, the electron mobility in the channel is much higher than in pure bulk GaAs with similar background doping. The alloy scattering is also important if the channel region is made of an alloy material such as InGaAs (Basu 1990). In the case of the AlGaAs/GaAs system, since the channel is formed in GaAs, and the penetration of the electron wavefunction into the AlGaAs region is quite small, the alloy scattering is insignificant. At very low temperatures, the acoustic phonon scattering also plays an important role. In modern well-designed structures, in which low temperature (≈ 10 K) mobilities over 10^6 cm^2/V s have been observed, the mobility is mainly limited only by this scattering mechanism. An excellent review of the mobility in HEMT structures is given by Mendez (1986).

4. New developments and areas of research

On the industrial scene, a number of leading laboratories around the world, including Fujitsu, Thomson–CSF, STL, AT&T, IBM, Rockwell, Hewlett–Packard, Hughes (to name a few) are actively engaged in the development of LSI circuits using HEMT. In particular, mention may be made of Fujitsu's projection to build a 10 K gate array with a propagation delay ≈ 100 ps/gate and a 16 K SRAM by 1992 (Mimura *et al* 1987). An excellent account of the current status of the ultra-high-speed HEMT technology has been given by Abe *et al* (1986). On the low noise microwave amplifiers side also, significant progress has been made both by Fujitsu and by Thomson–CSF, for applications in satellite communication. In parallel with these developments HEMT is also used in many academic and industrial laboratories for the study of a number of research problems in the basic physics of semiconductors. The discovery of the fractional quantum Hall effect (Tsui *et al* 1982) is a classic example of the use of this device for fundamental studies. Apart from these applications, there is also a great deal of active research being carried out to improve the capabilities of this device, and some of these are briefly discussed below.

4.1 *p-Modulation doping*

A two-dimensional hole gas (2-DHG) may be formed at the interface between GaAs and *p*-type AlGaAs using the valence band discontinuity. However, since the valence band discontinuity for this heterojunction is a smaller fraction of the band gap difference, the AlAs mole fraction (in *p*-AlGaAs) required to confine an appreciable concentration of holes in the *p*-quantum well is slightly larger. Using a $Al_{0.7}Ga_{0.3}As$: Be/GaAs *p*-modulation doped structures, a 2-DHG concentration of $\approx 6 \times 10^{11}\ cm^{-2}$ and a mobility of 32,000 cm^2/Vs at 4·2 K have been reported (Stormer *et al* 1984). The main interest in these *p*-channel devices is for the development of complimentary logic circuits using HEMT analogous to Si in CMOS circuits.

4.2 *Inverted HEMT*

The HEMT device structure (described in earlier sections) with Si-doped AlGaAs on the top of undoped GaAs is called a normal HEMT structure. If, on the other hand, the growth sequence is reversed (i.e. the Si-doped AlGaAs is grown first, and then the GaAs well region is grown), it is found that the electron mobility of these so-called 'inverted HEMT' structures is not as good as in the normal HEMT structures. The reason for this difference in behaviour was not understood for a long time, until it was shown (Inoue *et al* 1985) that Si-segregation from the AlGaAs into the GaAs channel region is responsible for the degradation of mobility in the inverted HEMT structures. By lowering the growth temperature to about 530°C, Inoue *et al* (1985) could overcome the problem of Si segregation, and demonstrate good electron mobilities in the inverted HEMT structures also.

4.3 *Double heterojunction HEMT*

With the successful fabrication of the inverted HEMT, the next logical step was to combine both the normal and inverted HEMT structures together in one device to get a larger concentration of the 2-DEG. This is realised in the double heterojunction HEMT formed by sandwiching a thin layer (≈ 300 Å) of undoped GaAs between two Si-doped AlGaAs layers separated by thin undoped AlGaAs spacer layers on either side. A typical cross-section of the device and its band diagram along the growth direction are shown in figures 7a and b. Charge control is achieved by making a Schottky gate on the top AlGaAs in the usual manner. A sheet electron concentration $\approx 2 \times 10^{12}\,\mathrm{cm}^{-2}$ and 77 K mobility of $\approx 60{,}000^2/\mathrm{V\,s}$ have been reported using this device (Inoue and Sakaki 1984). Using the alternative approach of replacing Si-doped AlGaAs by (Al,Ga)As/GaAs or AlAs/GaAs superlattices in which the dopants are placed only in GaAs, Arnold and co-workers have also successfully fabricated both inverted and double HEMT structures (Arnold *et al* 1984). Because of the larger sheet concentration attainable using double heterojunction HEMT, the current drivability of these devices is also large and hence they show much promise for high speed digital applications.

4.4 *New material systems*

Research efforts are currently under way to grow HEMT structures using other material systems which have higher electron mobility and/or saturation velocity, or have the potential for higher sheet charge concentration, or any other advantage.

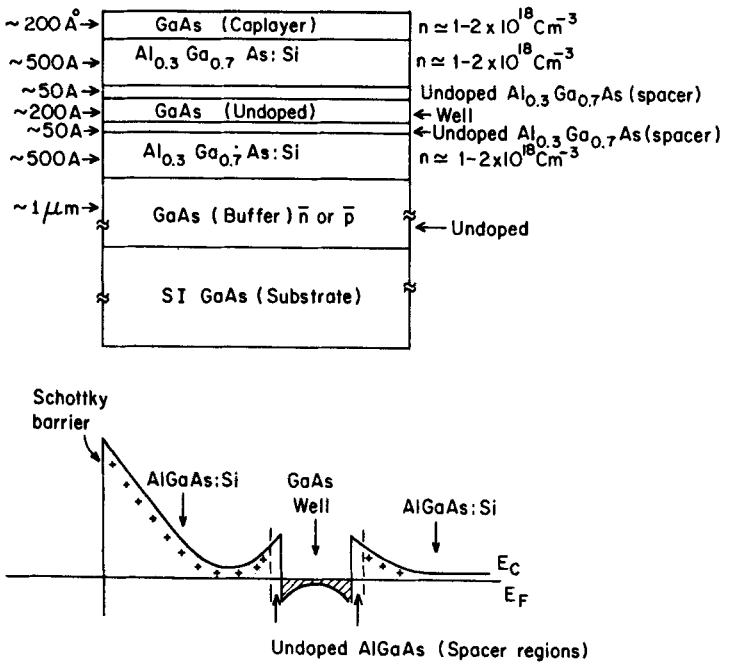

Figure 7. Schematic of the cross-section (**a**) and the band diagram in the growth direction (**b**) of a typical double heterojunction HEMT.

Two such systems which are highly promising at present are – (i) InAlAs/InGaAs, in view of the higher mobility in InGaAs (Kastalsky *et al* 1982), and (ii) (Si,Ge)/Si, in view of the highly advanced Si technology (People *et al* 1984). However, these materials are still in very preliminary stages of development, and more work is needed before useful devices could be produced with them.

4.5 *Problems due to the DX centres*

The single most important problem that still remains to be solved in the case of HEMT made from AlGaAs/GaAs system arises from the so-called *DX* centres in AlGaAs. These are defects related to the main donor itself (e.g. Si). It is well-known that all the so-called shallow donors in GaAs (Si, Sn, Te, Se etc.) become deep ($E_t \approx 0{\cdot}1$–$0{\cdot}15$ eV) in $Al_xGa_{1-x}As$ for $x > 0{\cdot}2$, and they couple very strongly to the lattice. They are associated with the phenomenon of persistent photoconductivity (PPC) observed in AlGaAs at low temperatures ($T < 100$ K), believed to be caused by a charge state dependent lattice relaxation around the defect (Lang *et al* 1979). The PPC effect is also observed in HEMT structures, which makes the device characteristics quite sensitive to (ambient) light at low temperatures (≈ 77 K). This is an undesirable effect since the real advantages of the HEMT lie in their low temperature operation. The *DX* centres in AlGaAs also give rise to a variety of other effects such as threshold voltage shifts with temperature (Valois *et al* 1983; Subramanian *et al* 1985; Subramanian 1985), drain current transients (Valois and Robinson 1983), collapse of the drain I–V characteristics at low temperatures in the dark (Fischer *et al* 1984) etc. This is a very active research field, and these studies have not only helped us to understand the effects of *DX* centres on HEMT, but also obtain a good deal of information about the *DX* centres themselves (Mooney *et al* 1987). This is an excellent example of a field in which technology and basic research have helped each other.

5. New proposed structures

5.1 *Velocity modulation transistor*

An HEMT, like any other field effect transistor, operates on the principle of modulation of the charge in the channel by a gate voltage, with the mobility in the channel being constant. This operation involves physically adding/removing charges to/from the channel, which in turn is limited by the transit time of the carrier in the channel. This places an ultimate limit on the speed of operation of HEMT to ≈ 1 ps, with present day technological constraints (imposed by lithography and material parameters). However, another form of modulation of the channel conductance is possible in principle, viz. modulating the carrier mobility in the channel by a gate voltage, keeping the total charge in the channel constant. This form of modulation can be extremely fast since charges are not physically added or removed, and the modulation of mobility can be brought about in a time constant comparable to the relaxation time of the carriers. A device that would operate on this principle is called a velocity modulation transistor (Sakaki 1982). Though such a device is yet to be practically realized, modulation of mobility up to 60% (i.e.

$\Delta\mu/\mu = 60\%$) in HEMT structures using front gate and back gate operations have been demonstrated (Hirakawa *et al* 1985). It has been predicted that by using a double heterojunction HEMT with an asymmetrical impurity distribution, it should be possible to modulate the mobility all the way from 4×10^3 cm^2/V s to 2×10^5 cm^2/V s and a switching time ≈ 200 fs should be possible with a well width ≈ 400 Å.

5.2 *One-dimensional structure*

In one-dimension (quantum well wire), an electron with a wave-vector k can be scattered only to a state $-k$ by Coulomb scattering (elastic). This makes the probability of scattering very low leading to theoretical mobilities $\approx 10^7$–10^8 cm^2/V s. A number of possible device structures using such one-dimensional wires have been proposed (Sakaki 1986) and the practical realization of such structures, and a number of interesting phenomena from such devices might be expected in the future.

6. Conclusions

A brief review of the basic physics of the high electron mobility transistor (HEMT) and the technological steps involved in the fabrication of the device are presented. Some preliminary results obtained in our laboratory in the fabrication of a test pattern containing a few transistors, a gated Van der Pauw structure etc. on an HEMT wafer are also included. Finally, the current status of the field, the problems remaining, the areas of active research and some of the proposed new structures are also briefly reviewed.

Acknowledgements

The author wishes to express his gratitude to Prof. J R Arthur, Oregon State University, Corvallis, USA with whom he initially started working in this field, and for the MBE-grown HEMT wafer provided by him. He is also indebted to his colleagues Dr B M Arora, Dr A S Vengurlekar, Dr A A Diwan, Mr V T Karulkar and to Dr K Chalapathy, Mr P P Suratkar and Ms B Lakshmi (SAMEER) for their contribution to some of the work described here.

References

Abe M, Mimura T, Shibatomi A and Kobayashi M 1986 *IEEE J. Quantum Electron.* **QE-22** 1870

Arnold D, Henderson T, Klem J, Fischer R, Kopp W, Ketterson A, Masselink W T and Morkoc H 1984 *Appl. Phys. Lett.* **45** 902

Basu P K 1990 *Bull. Mater. Sci.* **13** 65

Delagebeaudeuf D and Linh N T 1982 *IEEE Trans. Electron. Devices* **ED-29** 955

Dilorenzo J V, Dingle R, Feuer M, Gossard A C, Hendel R, Huang J C M, Kastalky A, Keramidas V G, Kiehl R A and O'Connor P 1982 *IEDM Tech. Dig.* 578

Dingle R, Stormer H, Gossard A C and Wiegmann W 1978 *Appl. Phys. Lett.* **31** 665

Drummond T J, Morkoc H and Cho A Y 1981 *J. Appl. Phys.* **50** 1380

Drummond T J, Morkoc H, Lee K and Shur M 1982 *IEEE Electron. Device Lett.* **EDL-3** 338

Drummond T J, Fischer R, Su S L, Lyons W G and Morkoc H 1983 *Appl. Phys. Lett.* **42** 262
Esaki L and Tsu R 1969 IBM Internal Research Report RC 2418
Fischer R, Drummond T J, Klem J, Kopp W, Henderson T S, Perrachione D and Morkoc H 1984 *IEEE Trans. Electron. Devices* **ED-31** 1028
Hirakawa K, Sakaki H and Yoshino J 1984 *Appl. Phys. Lett.* **45** 253
Hirakawa K, Sakaki H and Yoshino J 1985 *Phys. Rev. Lett.* **54** 1279
Inoue K and Sakaki H 1984 *Jpn. J. Appl. Phys.* **23** L61
Inoue K, Sakaki H, Yoshino J and Yoshioka Y 1985 *Appl. Phys. Lett.* **46** 102
Judaprawira S, Wang W I, Chao P C, Wood C E C, Woodard D W and Eastman L F 1981 *IEEE Electron. Device Lett.* **EDL-2** 14
Kastalsky A, Dingle R, Chang K Y and Cho A Y 1982 *Appl. Phys. Lett.* **41** 274
Lang D V, Logan R A and Jaros M 1979 *Phys. Rev.* **B-19** 1015
Lee C P, Miller D L, Hou D and Anderson R J 1983a *IEEE Trans. Electron. Devices* **ED-30** 1569
Lee K, Shur M S, Drummond T J and Morkoc H 1983b *J. Appl. Phys.* **54** 2093
Lee K, Shur M S, Drummond T J and Morkoc H 1983c *IEEE Trans. Electron. Devices* **ED-30** 207
Lee K, Shur M S, Drummond T J, Su S L, Lyons W G, Fischer R and Morkoc H 1983d *J. Vac. Sci. Technol.* **B1** 186
Linh N T, Tung P N, Delagebeaudeuf D, Deslesinse P and Laviran M 1982 *IEDM Tech. Dig.* 582
Mendez E E 1986 *IEEE J. Quantum Electron.* **QE-22** 1720
Mimura T, Joshin K, Hiyamizu S, Hikosaka K and Abe M 1981 *Jpn. J. Appl. Phys.* **20** L598
Mimura T, Abe M, Komeno J and Kondo K 1987 *Physics of semiconductor devices* (eds) S C Jain and S Radhakrishna (Singapore: World Scientific) p. 58
Mooney P M, Caswell N S and Wright S L 1987 *J. Appl. Phys.* **62** 4786
Morkoc H 1981 *IEEE Electron. Device Lett.* **EDL-2** 260
Morkoc H 1985 in *Molecular beam epitaxy and heterostructure* (eds) L Chang and K Ploog (The Hague: Martinus Nijhoff.) p. 625
People R, Bean J C, Lang D V, Sergent A M, Stormer H L, Wecht K W, Lynch R T and Baldwin K 1984 *Appl. Phys. Lett.* **45** 1231
Pierret R F and Lundstrom M S 1984 *IEEE Trans Electron Devices* **ED-31** 383
Sakaki H 1982 *Jpn. J. Appl. Phys.* **21** L381
Sakaki H 1986 *IEEE J. Quantum Electron.* **QE-22** 1845
Solomon P and Morkoc H 1984 *IEEE Trans. Electron. Devices* **ED-31** 1015
Stormer H L, Dingle R, Gossard A C, Wiegmann W and Sturge M D 1979 *Solid State Commun.* **29** 705
Subramanian S 1985 *IEEE Trans. Electron. Devices* **ED-32** 865
Subramanian S, Schuller U and Arthur J R 1985 *J. Appl. Phys.* **58** 845
Subramanian S, Vengurlekar S and Diwan A A 1986 *IEEE Trans. Electron. Devices* **ED-33** 707
Tsui D C, Stormer H L and Gossard A C *Phys. Rev. Lett.* **48** 1559
Valois A J and Robinson G Y 1983 *IEEE Electron. Devices Lett.* **EDL-4** 360
Valois A J, Robinson G Y, Lee K and Shur M S 1983 *J. Vac. Sci. Technol.* **B1** 190
Vinter B 1984 *Appl. Phys. Lett.* **44** 307